HYDROLOGIC SENSITIVITY OF GLOBAL RIVERS TO CLIMATE CHANGE

BART NIJSSEN, GREG M. O'DONNELL, ALAN F. HAMLET and DENNIS P. LETTENMAIER
Department of Civil and Environmental Engineering, Box 352700, University of Washington, Seattle, WA 98195-2700, U.S.A.
E-mails: nijssen@u.washington.edu, tempgd@hydro.washington.edu, hamleaf@u.washington.edu, and dennisl@u.washington.edu

Abstract. Climate predictions from four state-of-the-art general circulation models (GCMs) were used to assess the hydrologic sensitivity to climate change of nine large, continental river basins (Amazon, Amur, Mackenzie, Mekong, Mississippi, Severnaya Dvina, Xi, Yellow, Yenisei). The four climate models (HCCPR-CM2, HCCPR-CM3, MPI-ECHAM4, and DOE-PCM3) all predicted transient climate response to changing greenhouse gas concentrations, and incorporated modern land surface parameterizations. Model-predicted monthly average precipitation and temperature changes were downscaled to the river basin level using model increments (transient minus control) to adjust for GCM bias. The variable infiltration capacity (VIC) macroscale hydrological model (MHM) was used to calculate the corresponding changes in hydrologic fluxes (especially streamflow and evapotranspiration) and moisture storages. Hydrologic model simulations were performed for decades centered on 2025 and 2045. In addition, a sensitivity study was performed in which temperature and precipitation were increased independently by 2 °C and 10%, respectively, during each of four seasons. All GCMs predict a warming for all nine basins, with the greatest warming predicted to occur during the winter months in the highest latitudes. Precipitation generally increases, but the monthly precipitation signal varies more between the models than does temperature. The largest changes in the hydrological cycle are predicted for the snow-dominated basins of mid to higher latitudes. This results in part from the greater amount of warming predicted for these regions, but more importantly, because of the important role of snow in the water balance. Because the snow pack integrates the effects of climate change over a period of months, the largest changes occur in early to mid spring when snow melt occurs. The climate change responses are somewhat different for the coldest snow dominated basins than for those with more transitional snow regimes. In the coldest basins, the response to warming is an increase of the spring streamflow peak, whereas for the transitional basins spring runoff decreases. Instead, the transitional basins have large increases in winter streamflows. The hydrological response of most tropical and mid-latitude basins to the warmer and somewhat wetter conditions predicted by the GCMs is a reduction in annual streamflow, although again, considerable disagreement exists among the different GCMs. In contrast, for the high-latitude basins increases in annual flow volume are predicted in most cases.

1. Introduction

There is a growing consensus in the geoscience community that the Earth will experience a gradual warming in the coming decades, the major cause of which is continuing increases in global concentrations of so-called greenhouse gases. Burn-

Climatic Change **50:** 143–175, 2001.
© 2001 *Kluwer Academic Publishers. Printed in the Netherlands.*

ing of fossil fuels, in particular, is likely to continue to increase atmospheric CO_2 concentrations to more than double their pre-industrial levels within the next 100 years (IPCC, 1996). In the past few years, the focus of research related to climate change has shifted from the question whether global warming will occur to understanding where and how much change is likely to occur. In the United States, for example, the U.S. National Assessment of Climate Variability and Change (hereafter USNA) is assessing the potential impacts of climate variability and change on 20 regions and five sectors throughout the U.S. One of the five sectors addressed by the USNA is water resources.

Changes in atmospheric circulation, as evidenced by fluxes of moisture and energy at the land surface, have immediate as well as long-term effects on river systems. At short time scales, from days to months, changes in weather patterns can lead to changes in the incidence of floods. At longer time scales, from seasons to years, changes in drought characteristics are the main hydrologic manifestation of climate change. At annual to decadal time scales, teleconnections in global atmospheric circulation patterns, caused primarily by ocean-atmosphere interactions, strongly affect the hydrology of certain regions, especially in the tropics, but also in some extra-tropical regions (e.g., Battisti and Sarachik, 1995; Glanz et al., 1991). For example, the El Niño/Southern Oscillation (ENSO) has been linked to floods and drought in Southern Africa (Thiaw et al., 1999), and precipitation anomalies in eastern Australia (Simpson et al., 1993).

Global increases in temperatures directly affect the hydrology of the land surface through changes in the accumulation and ablation of snow, as well as in evapotranspiration. Changes in atmospheric circulation are also predicted to result in changes in precipitation amounts, intensities and patterns (e.g., Felzer and Heard, 1999). Although most general circulation models (GCMs) predict increases in global average precipitation, there is little consensus on the amount or even direction of regional changes. On the other hand, almost all climate models show increases in temperature in most regions and for most seasons. Discrepancies in GCM predictions of temperature change are more in magnitude than in direction.

Changes in land surface hydrology due to changing climate, such as changes in the discharge of large, continental rivers, have potentially far reaching implications both for human populations and for regional-scale physical and ecological processes. The geographic and topographic characteristics of large river basins and the climatic variations that determine their hydrologic characteristics often constitute the defining features of the regions they occupy. They govern to a considerable extent the development of ecosystems, as well as human communities and their activities. These regional ecosystems and human activities are usually reasonably well adapted to the current climate conditions, but may be vulnerable to large or rapid changes in climate.

In industrialized nations, food supplies and human health are at least partially insulated from natural hydrologic variability. Where water is intensely managed, the implications of changing hydrologic characteristics can be considered in the

context of water management and associated institutional considerations. The Mississippi River has frequently been examined in this context (e.g., Olsen et al., 1999). In the developing world, the context is often very different, because even 'normal' variations in climate and streamflow can result in devastating floods in both urban and rural areas, or droughts that create potentially catastrophic food shortages. Serious human health problems frequently accompany both of these extremes.

Clearly, changes in climate are not the only cause of pressure on water resources. Vörösmarty et al. (2000) argue that 'impending global-scale changes in population and economic development over the next 25 years will dictate the future relations between water supply and demand to a much greater degree than will changes in mean climate'. Arnell (1999b) also investigated the changes in water resource stress as a result of predicted climate change and population growth. These socio-economic changes are outside the scope of this paper. However, we think that the results presented here can be an important source of information for such studies.

Most regional assessments of climate change impacts are based on coupled land-atmosphere-ocean simulations produced by GCMs. Because of the relatively coarse spatial resolution at which GCMs operate (typically several degrees latitude by longitude), downscaling and adjustment for model bias is essential for interpretation of regional change predictions (Lettenmaier et al., 1999; Hamlet and Lettenmaier, 1999; Doherty and Mearns, 1999; Leung et al., 1999). Nonetheless, GCMs do simulate the large scale features of global climate with some skill, and some have been shown to capture important climatic tele-connections (e.g., those associated with ENSO (Leung et al., 1999)).

Many studies of the impact of climate change on water resources for specific geographic regions have been reported. Gleick (1999), for example, describes an extensive bibliography with more than 800 papers about the impacts of climate change on U.S. water resources. Arnell (1999a) studied the effect of climate change on hydrological regimes in Europe. In contrast, this study attempts to place the regional hydrological consequences of climate predictions in a global context. We examine the hydroclimatic conditions under which sensitivities of key hydrologic variables, including streamflow, evaporation, snow storage and soil moisture, are greatest, and the relative implications of these hydrological sensitivities for water management.

Our assessment targets nine large river basins, selected to represent a range of geographic and climatic conditions. Changes in precipitation and temperature were calculated based on altered climate simulations produced by long (multi-decadal) runs of four GCMs. To enhance understanding of the causal relationships between changes in surface climatic variables (which constitute forcings for the land surface hydrologic system) and resulting changes in hydrologic conditions, we also conducted a set of sensitivity experiments in which temperature and precipitation were altered independently for each of the four seasons.

Table I
Selected river basins

River basin	Gauge location	Predominant climatic zones	Area (km^2) upstream of gauge [a]
Amazon	Obidos, Brazil	Tropical	4,618,746
Amur	Komsomolsk, Russia	Arctic Mid latitude – rainy	1,730,000
Mackenzie	Norman Wells, Canada	Arctic	1,570,000
Mekong	Pakse, Laos	Tropical	545,000
Mississippi	Vicksburg, U.S.A.	Mid latitude – rainy	2,964,254
Severnaya Dvina	Ust – Pinega, Russia	Arctic	348,000
Xi	Wuzhou, China	Mid latitude – rainy	329,705
Yellow	Huayuankou, China	Arid – cold Mid latitude – rainy	730,036
Yenisei	Igarka, Russia	Arctic	2,440,000

[a] Areas are taken from the GRDC and RivDis data bases.

2. Experimental Design

2.1. RIVER BASINS

Given the large scale of application and the conceptual nature of some parameterizations used in macroscale hydrological models (MHMs), some calibration of model parameters is inevitably necessary (Nijssen et al., 2001a). However, the calibration process is time-consuming and quickly becomes infeasible when the modeled area is large. To avoid this problem, Nijssen et al. (2001a) developed an approach for transferring model parameters from calibrated to uncalibrated river basins. As part of their study, the variable infiltration capacity (VIC (Liang et al., 1994; Nijssen et al., 1997)) MHM was implemented for 26 large river basins. These river basins were in turn a subset of the 50 continental-scale river basins delineated by Graham et al. (1999). The nine river basins selected for this study (Table I) are a subset of the 26 river basins studied by Nijssen et al. (2001a). They were selected on the basis of the performance of the VIC model and the desire to represent a range of climatic and geographic regions globally. Figure 1 shows the location of the nine river basins. For each basin, historic river discharge records were obtained from the Global River Discharge Center (GRDC) in Koblenz, Germany, and from the RivDis 1.1 data base (Vörösmarty et al., 1998).

Because of the paucity of data records in most of the tropics, the selected river basins are concentrated in the Northern Hemisphere. However, from a climate change perspective this is not necessarily problematic. The most prominent sig-

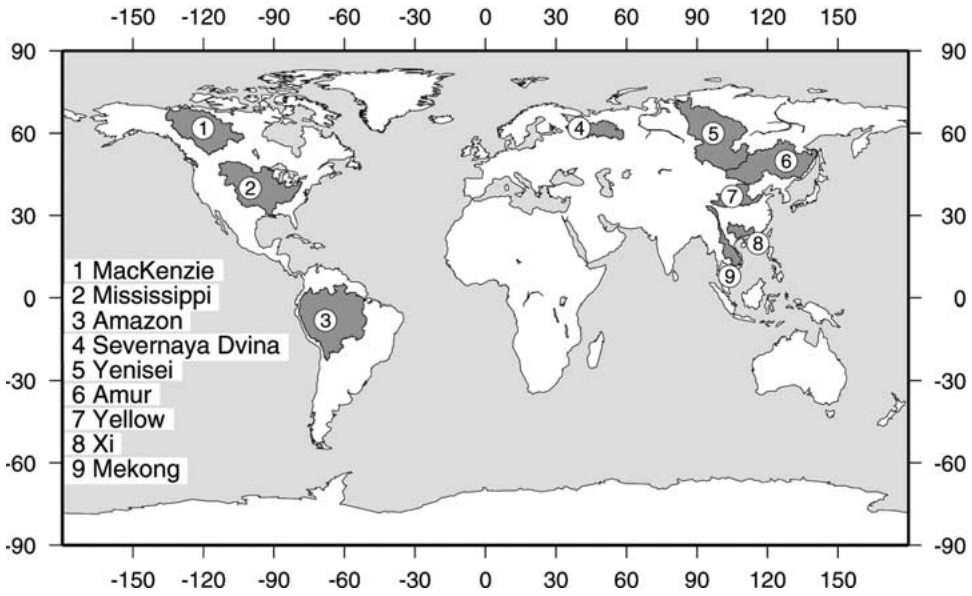

Figure 1. Location of the nine selected river basins.

nature of recent warming detected in long-term observations is during the winter over the high mid-latitudes of the Northern Hemisphere continents (Nicholls et al., 1996). Most climate models, including the ones used in this study, predict a similar signature. Nonetheless, as more data records for tropical regions become available, it would be of interest to further explore the hydrologic sensitivity of those river basins in more detail.

2.2. SPATIAL AND TEMPORAL SCALE

Many recent studies have examined the response of state-of-the-art GCMs to changing greenhouse gas concentrations and the effects of changes in water cycles on regional scale hydrologic processes, ecosystems, and water resources. Gleick (1999) summarizes a group of studies, performed for the USNA and included in a special issue of the Journal of the American Water Resources Association (a second special issue of the same journal was published in April 2000). These studies have been carried out at varying levels of spatial and temporal detail. Some insight into the implications of the spatial and temporal resolution of the results on the nature of the conclusions drawn from each can be gleaned from a review of these studies.

At continental spatial scales, Felzer and Heard (1999) examined future precipitation changes over North America simulated by two GCMs; Wolock and McCabe (1999) examined potential changes in mountain snow pack in the Western U.S.; while Frederick and Schwarz (1999) examined socio-economic impacts to regional water supplies in the U.S. At somewhat smaller regional spatial scales, several studies focused on more detailed hydrology and water resources impacts (Chao,

1999; Gleick and Chalecki, 1999; Hamlet and Lettenmaier, 1999; Ojima et al., 1999; Olsen et al., 1999). At fine spatial scales, Leung and Wigmosta (1999), and Miller et al. (1999) examined watershed response based on downscaling of GCM simulations using nested meso-scale climate models and high resolution distributed hydrology models for several small watersheds.

Each of these studies captures different climate and hydrologic effects. Large scale studies in some cases overlook seasonal or spatial distinctions that have important consequences. For example, Frederick and Schwarz (1999) reported socioeconomic impacts to Pacific Northwest (PNW) water resources based on annual increases in streamflow volumes. These impacts were almost certainly underestimated because reservoir storage in the Pacific Northwest is, in aggregate, much less than mean annual runoff, meaning that it tends to be more sensitive to seasonal patterns of runoff than to interannual variations. Frederick and Schwarz (1999) based their conclusions on predicted annual increases in streamflows, but did not consider the large changes in the seasonal patterns of runoff that would occur under global warming. Hamlet and Lettenmaier (1999) and Leung and Wigmosta (1999), on the other hand, also predicted modest annual increases in streamflow for the Pacific Northwest, but showed the importance of seasonal changes in streamflow patterns and of topographic features such as basin elevation, which strongly affect the timing of snowmelt, and hence runoff.

These results for the PNW suggest that studies of hydrologic sensitivity to climate change should at the least include consideration of possible seasonal hydrologic changes. Furthermore, the studies by Leung et al. (1999) and Hamlet and Lettenmaier (1999) suggest that MHMs are able to capture the effects of the dominant climate signals for large river basins. Except in situations where high-resolution, local interpretations of climatic sensitivities are required, MHMs should be sufficient for regional impact studies. The selection of the spatial and topographic scale of the modeling experiments described here are based on this premise.

2.3. DOWNSCALING

Despite rapid advances in the development of GCMs, their output generally shows significant biases in the simulation of both temperature and precipitation under current climate conditions. These biases are often so large that direct application of the modeled meteorology in a macroscale hydrological model is not meaningful (e.g., Doherty and Mearns, 1999).

Various methods have been used to downscale GCM results to hydrologically relevant spatial scales. One of the more appealing methods uses a nested regional climate model, which is forced at the boundary by the GCM, and which within its domain resolves spatial scales relevant to the hydrological model. The problem with this approach is that it is extremely computationally intensive and the results inherit biases not only from the global GCM, but also from the regional climate

model. The end result is invariably that the climate model output, downscaled or not, must be adjusted so that a 'base case' scenario, intended to represent the current climate, does in fact have the same statistical characteristics as the historical observations. Adjustments are commonly required to create a base case, relative to which alternative climate scenarios can be interpreted. A number of studies have tested various downscaling methods ranging from very simple interpolations (e.g., Lettenmaier and Gan, 1990) to rather complicated methods that are based on stochastic representation of the evolution of daily weather patterns, and their relationship to daily precipitation and temperature (Hughest et al., 1993).

The uncertainties of these past studies are based largely on the significant differences in climate change predictions between the different GCMs. For the present, we therefore conclude that the simplest methods that impose the seasonal cycle of regional-scale, GCM-predicted average changes on an observed temperature and precipitation record are sufficient to investigate the range of hydrologic responses. Accordingly, predicted changes in precipitation and temperature were applied as a basin-wide, monthly average change. These changes were calculated as mean monthly changes between a GCM control run and a particular decade in a transient GCM run. The CO_2 (or equivalent greenhouse gas) concentration is kept constant in the control run (at historic levels in most cases) and is increased in the transient runs according to a specified emission scenario. Precipitation changes were defined as the relative change in aggregated precipitation volume over the basin, while temperature changes were defined as a shift in average temperature over the basin.

2.4. CLIMATE MODELS AND EMISSION SCENARIOS

Climate scenarios from eight different GCMs were obtained from the Intergovernmental Panel on Climate Change Data Distribution Center (IPCC DDC) (Table II). All eight models are coupled ocean-atmosphere models, output from which was archived as part of the IPCC climate change efforts. Four of these models (CCCMA-CGCM1, HCCPR-CM2, MPI-ECHAM4, and DOE-PCM3) were also used as part of the U.S. National Assessment. The models differ in the spatial resolution and the processes they represent. Most of the models simulate a change in greenhouses gases by changing the CO_2 concentration in the atmosphere, using an equivalent CO_2 concentration, instead of explicit representation of the individual greenhouse gases. Only two of the models (HCCPR-CM3 and DOE-PCM3) simulate the effects of a number of individual greenhouse gases explicitly. These two models are also the only two models that do not use a flux correction to account for biases in the energy and moisture fluxes between the atmosphere and ocean. Four of the models use bucket-type land surface schemes to simulate land surface hydrology, while the other four use more modern, explicit representations of vegetation and incorporate more sophisticated runoff generation mechanisms.

The transient emission scenarios differ slightly between the models (Table II), partly because the models represent greenhouse gas chemistry differently. The

Table II
Selected climate models and scenarios

Organization	Model	Model resolution lat. × lon.	Land surface scheme	Flux corrected?	Transient emission scenario [a]	Reference
CCCMA Canadian Centre for Climate Modelling and Analysis, Canada	CGCM1	3.75° × 3.75°	Bucket	Yes	A	Boer et al. (2000a,b)
CCSR Center for Climate Research Studies, Japan	CCSR CGCM	5.5° × 5.5°	Bucket	Yes	B	Emori et al. (1999)
CSIRO Commonwealth Scientific and Industrial Research Organisation, Australia	CSIRO CGCM	3.2° × 5.6°	Bucket	Yes	B	Gordon and O'Farrell (1997)
GFDL Geophysical Fluid Dynamics Laboratory, U.S.A.	GFDL CGCM	4.5° × 7.5°	Bucket	Yes	A	Manabe et al. (1991) Stouffer and Manabe (1999)
HCCPR Hadley Center for Climate Prediction and Research, U.K.	CM2	2.5° × 3.75°	Vegetation and runoff	Yes	A	Johns et al. (1997)
HCCPR Hadley Centre for Climate Prediction and Research, U.K.	CM3	2.5° × 3.75°	Vegetation and runoff	No	C	Gordon et al. (2000)
MPI Max Planck Institute for Meteorology, Germany	ECHAM4	2.8° × 2.8°	Vegetation and runoff	Yes	B	Röckner et al. (1996) Röckner et al. (1999)
DOE Department of Energy, U.S.A.	PCM3	2.8° × 2.8°	Vegetation and runoff	No	C	Washington et al. (2000)

[a] The transient model scenarios are grouped as follows: A: 1% annual increase in equivalent CO_2, and sulphate aerosols according to IS92a; B: Equivalent CO_2 and sulphate aerosols according to IS92a; C: Increase in several greenhouse gases and sulphate aerosols according to IS92a.

three different emission scenarios used are: (a) 1% annual increase in equivalent CO_2 and sulphate aerosols according to the IPCC IS92a scenario (A); (b) equivalent CO_2 and sulphate aerosols according to IS92a (B); and (c) several greenhouse gases (including CO_2) and sulphate aerosols according to IS92a (C). The IS92a scenario is one of the emission scenarios specified by IPCC and gives a doubling of equivalent CO_2 after about 95 years (IPCC, 1996). A 1% annual increase in equivalent CO_2 (doubling in 70 years) results in a 20% higher radiative forcing for a given future time horizon compared to the IS92a scenario (IPCC, 1996).

Figure 2 shows the predicted changes in mean annual temperature and precipitation for each of the nine basins for the decades 2020–2029, 2040–2049, and 2090–2099. These decades will hereafter be referred to as 2025, 2045, and 2095, respectively. All models predict a progressive warming for all basins, but the amount of warming for each basin differs by model. Not unexpectedly, the spread between the models increases with an increase in the lead time of the prediction. Some of the differences are likely attributable to the differences in the emission scenarios, although there is no clear difference in warming signal between the models that use scenario A and those that use scenarios B and C. Predicted annual average warming ranges from 0.8 °C for the Xi (HCCPR-CM2) to 4.2 °C for the Mackenzie (CCSR-CGCM) in 2025, from 1.1 °C for the Yenisei (DOE-PCM3) to 4.9 °C for the Mackenzie (CCSR-CGCM) in 2045, and from 2.5 °C for the Xi (DOE-PCM3) to 8.5 °C for the Mackenzie (CCSR-CGCM) in 2095. All models predict an increase of precipitation for the northern basins (Mackenzie, Severnaya Dvina and Yenisei), but the signal is mixed for basins in the mid-latitudes and tropics, although on average slight precipitation increases are predicted. Predicted changes in precipitation range from –16.5% for the Xi (CCCMA-CGCM) to 15.0% for the Mackenzie (CSIRO-CGCM) in 2025, from –15.9% for the Xi (CCCMA-CGCM) to 14.3% for the Severnaya Dvina (GFDL-CGCM) in 2045, and from –30.3% for the Xi (CCCMA-CGCM) to 27.6% for the Mackenzie (CSIRO-CGCM) in 2095. The CCCMA-CGCM model generally predicts the largest decrease in precipitation and for many basins also the largest increase in temperature, especially in 2095.

In the remaining part of this study we will focus on the results of four of the climate models (HCCPR-CM2, HCCPR-CM3, MPI-ECHAM4, and DOE-PCM3) and on two decades (2025 and 2045). These four models were selected because they offer the greatest spatial resolution, facilitating the downscaling step to the $2^\circ \times 2^\circ$ resolution of the hydrology models. More importantly, these four models include modern and relatively sophisticated land surface schemes that represent explicitly the interactions between vegetation and the surface energy and moisture budgets. The decades 2025 and 2045 were selected for two reasons. First, in 2095 the spread in the predicted changes in temperature and precipitation is much larger than in the other two decades and some of the predicted changes in temperature are very large, even for these four models (e.g., 7.0 °C warming for the Amazon in 2095 (HCCPR-CM3)). Second, planning horizons in water resources development

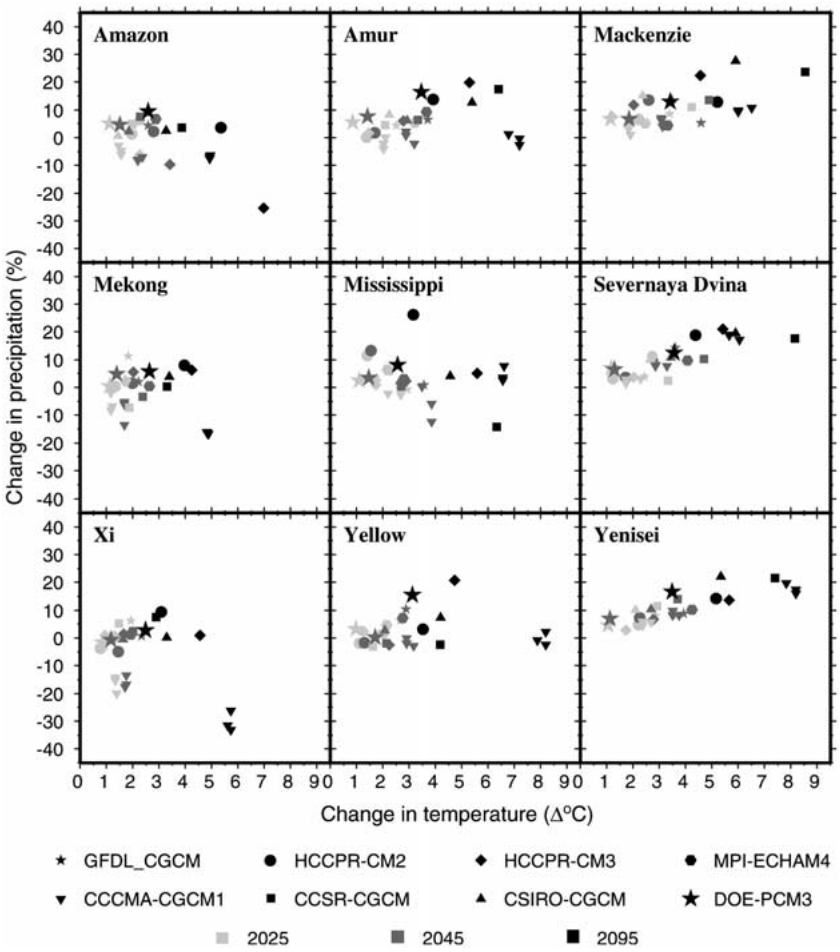

Figure 2. Predicted changes in mean annual temperature and precipitation for each river basin for the decades 2020–2029 (2025), 2040–2049 (2045), and 2090–2099 (2095). Note that climate prediction for 2095 were not available for GFDL-CGCM and MPI-ECHAM4. Also note that the CCCMA-CGCM model provided three ensemble runs, all three of which are plotted.

are more typically on the order of 20–30 years, placing a greater emphasis on the decades 2025 and 2045.

2.5. VARIABLE INFILTRATION CAPACITY MODEL

The predicted changes in temperature and precipitation, that is, the mean monthly differences between the GCM transient and control runs, were used to perturb observed temperature and precipitation records. Both the historical and the perturbed records were used to drive a MHM to study the hydrological effects of changes in atmospheric forcings. The MHM used in this study is the variable infiltration capacity (VIC) model (e.g., Liang et al., 1994, 1996; Nijssen et al., 1997). The

VIC MHM has been used in a number of modeling studies of large river basins (e.g., Abdulla et al., 1996; Cherkauer and Lettenmaier, 1999; Lohmann et al., 1998b; Matheussen et al., 2000; Nijssen et al., 1997, 2001a,b; Wood et al., 1997). Distinguishing characteristics of the VIC model include the representation of:

- subgrid variability in land surface vegetation classes;
- subgrid variability in the soil moisture storage capacity, which is represented as a spatial probability distribution;
- subgrid variability in topography through the use of elevation bands;
- drainage from the lower soil moisture zone (baseflow) as a nonlinear recession;
- spatial subgrid variability in precipitation.

The VIC model calculates the moisture fluxes for each model grid cell independently. Because the model grid cells are large ($2^\circ \times 2^\circ$), it is assumed that there is no significant exchange of ground water between the cells. The generated daily baseflow and 'fast response' runoff are routed downstream using a stand-alone routing model, which is described in detail by Lohmann et al. (1996, 1998a). Streamflow can exit each grid cell in eight directions and all flow must exit in the same direction. The flow from each grid cell is weighted by the fraction of the grid cell that lies within the basin. As in Nijssen et al. (2001a,b) flows were routed on a $1^\circ \times 1^\circ$ network, because the higher resolution flow networks allowed a somewhat better approximation of the modeled channel network than the native $2^\circ \times 2^\circ$ spatial resolution.

In the context of the climate change simulations it should be noted that the VIC model does not include CO_2 enrichment effects. Although the direct effects of increased temperatures and CO_2 concentrations on plant growth are reasonably well understood individually, their combined outcome is unclear and merits more study (Kirschbaum et al., 1996; Melillo et al., 1996). Similarly, climate-induced vegetation changes were not considered in the model experiments, and all model runs were executed using the baseline vegetation.

2.6. BASELINE SIMULATION

The baseline simulation acts as a surrogate for the real system under current climate conditions. In the baseline simulation the VIC model was forced with observed temperature and precipitation. This allowed a comparison between modeled and observed hydrographs to ensure that the MHM can capture and replicate the important hydrological processes. Subsequently, all changes in hydrological fluxes and storages were calculated relative to this baseline simulation. Results from previous work by Nijssen et al. (2001a,b) were used for the baseline simulations.

In Nijssen et al. (2001b), a gridded data set of daily meteorological model forcings for the period 1979–1993 was developed for global land areas (excluding Greenland and Antarctica) at a spatial resolution of $2^\circ \times 2^\circ$. Daily precipitation and

daily minimum and maximum temperature were derived from station observations, and extended using stochastic interpolation methods for those areas with insufficient coverage by daily meteorological stations. The resulting daily sequences were scaled to match the means of pre-existing global, monthly time series (Hulme, 1995; Huffman et al., 1997; Jones, 1994). Daily surface wind speeds were obtained from the NCEP/NCAR reanalysis project (Kalnay et al., 1996). The remaining meteorological forcings (vapor pressure, incoming shortwave radiation, and net longwave radiation) are calculated by the VIC model based on daily temperature and precipitation using algorithms by Kimball et al. (1997), Thornton and Running (1999), and Bras (1990).

The daily data were used to drive the VIC model to calculate a set of derived variables (evapotranspiration, runoff, snow water equivalent, and soil moisture) and to study the water balance of each of the continents. For each $2^\circ \times 2^\circ$ model grid cell land surface characteristics such as elevation, soil and vegetation were specified. Elevation data were calculated based on the 5 minute TerrainBase Digital Elevation Model (DEM) (Row et al., 1995), using the land surface mask from Graham et al. (1999). Vegetation types were provided by the AVHRR-based, 1 km, global land classification from Hansen et al. (2000), which has 12 unique vegetation classes. Vegetation parameters such as height and minimum stomatal resistance were assigned to each individual vegetation class. Soil textural information and soil bulk densities were derived from the five minute FAO-UNESCO digital soil map of the world (FAO, 1995), combined with the WISE pedon data base (Batjes, 1995). The remaining soil characteristics, such as porosity, saturated hydraulic conductivity, and the exponent for the unsaturated hydraulic conductivity equation were based on Cosby et al. (1984).

As discussed in Section 2.1, Nijssen et al. (2001a) used the same (base case) data and model to evaluate methods for model parameter transfer from calibrated to uncalibrated basins. The final calibrated flows for the nine selected basins (which were taken from Nijssen et al. (2001a)) had a mean absolute bias in the annual flow volume of 10.0% and a mean relative root mean squared error of the monthly discharge time series of 40.6%. The mean monthly hydrographs of observed and simulated flow are shown in Figure 3. We again emphasize that in the remainder of this paper, when examining the hydrologic effects of altered climate scenarios, the change in the hydrologic fluxes were calculated relative to the results from the baseline simulation, rather than the historic observations. This convention avoids, at least to first order, the effects of model bias.

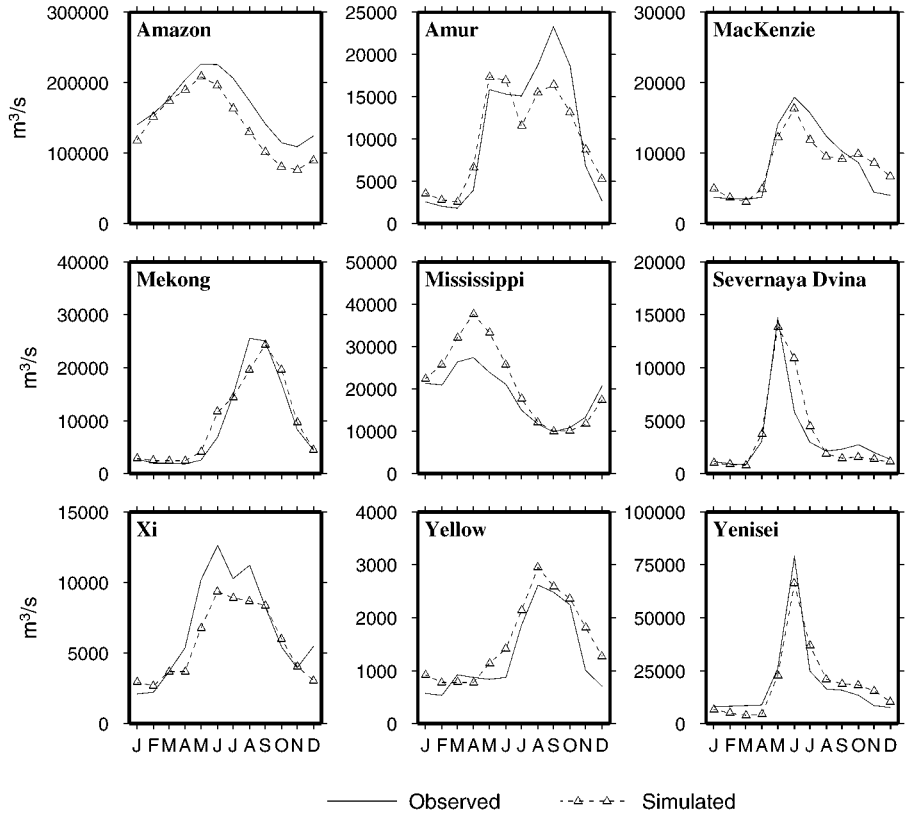

Figure 3. Mean monthly observed and simulated hydrographs for the period 1980–1993 (note that mean flows were only calculated based on those months for which coincident simulated and observed values were available).

3. Climate Scenarios

3.1. PRECIPITATION AND TEMPERATURE CHANGES

Figures 4 and 5 show the baseline mean monthly temperature and precipitation, with superimposed predicted monthly changes in temperature (in °C) and precipitation (in percent) for the four climate models for 2045. Changes in 2025 (not shown) are similar, but are generally smaller in magnitude.

All rivers other than the Amazon have a strong seasonal temperature signal, with a maximum in July and August. As expected, the amplitude of the seasonal temperature cycle increases with latitude. Generally, the increases in temperature for the tropical and mid-latitude basins (Amazon, Mekong, Xi and Mississippi) are fairly evenly distributed throughout the year. For the high-latitude basins, the temperature increases have a strong seasonal signal for most of the models, with the largest increases in temperature predicted for the winter months. However, there

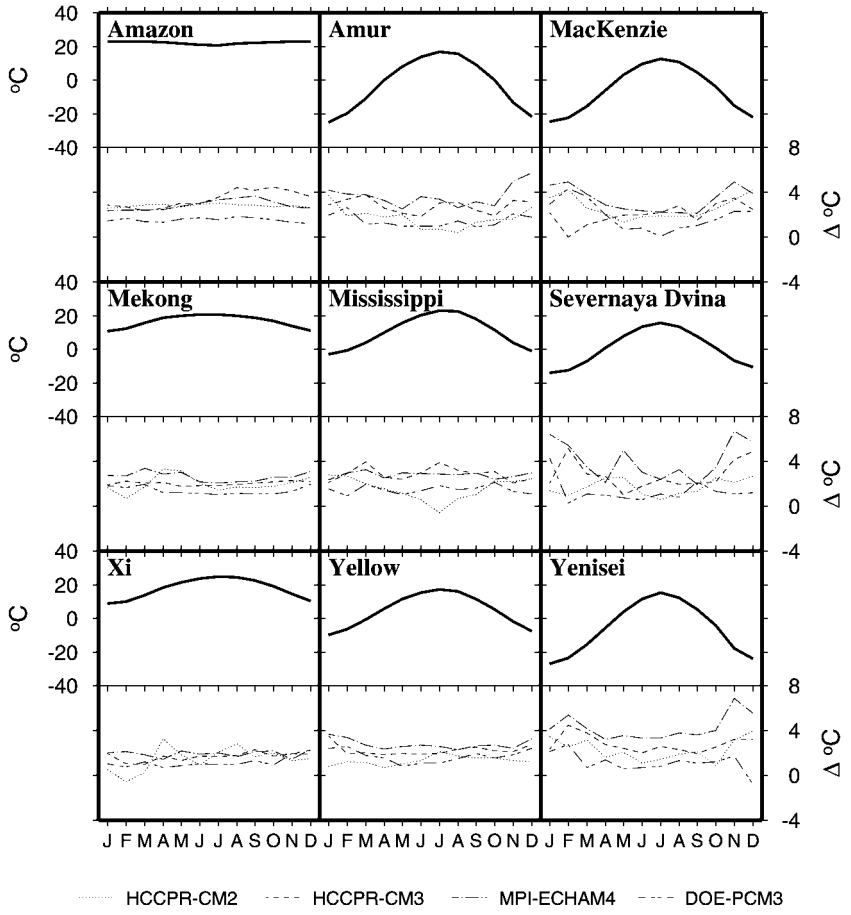

Figure 4. Baseline and predicted changes in temperature for 2045.

is considerable variation in the change predicted by the GCMs, especially on a monthly basis.

The predicted relative changes in precipitation likewise have their largest increases during the winter months for high-latitude basins. Note however, that in some of these basins the precipitation falls mainly in the summer, and a small relative change in summer might amount to a larger change in annual precipitation volume than a large relative change in winter. For example, most of the climate models show increased precipitation for the Yellow River during fall, winter and spring, but a decrease during the summer months. Because most of the precipitation in the Yellow river basin falls during these summer months, the net effect is a decrease in annual precipitation in 2045 for two models (HCCPR-CM2 and HCCPR-CM3), no change for one model (DOE-PCM3) and a small increase for the fourth model (MPI-ECHAM4). The opposite is the case for the Mekong River, where an increase of precipitation is predicted during the monsoon season, and

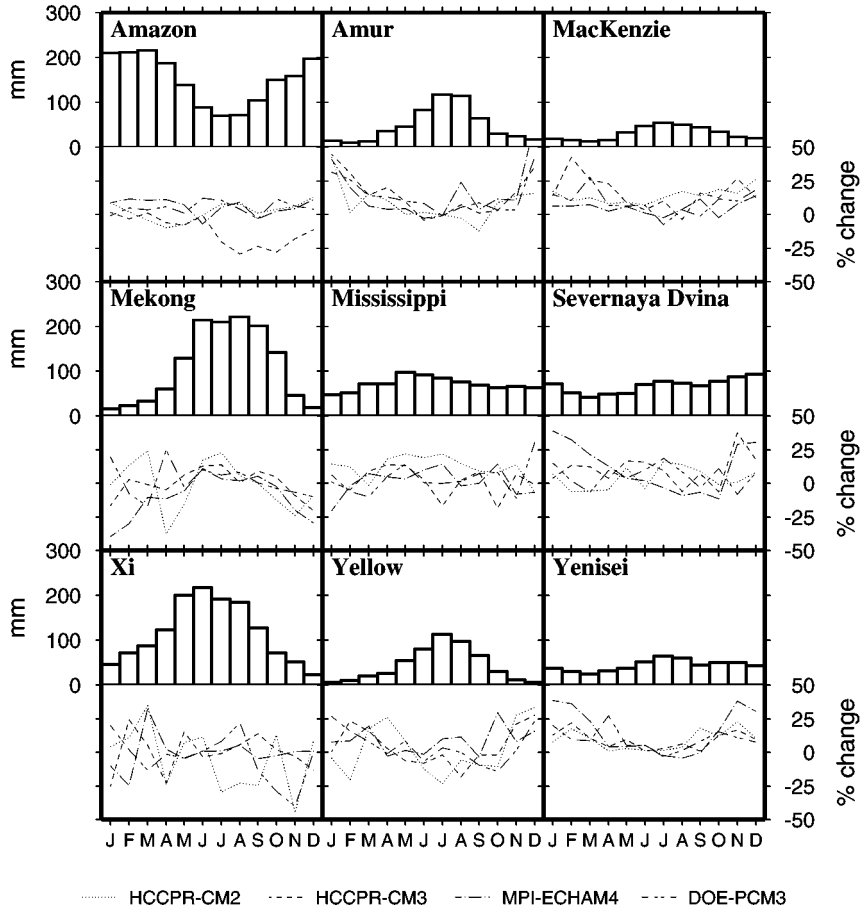

Figure 5. Baseline and predicted changes in precipitation for 2045.

a decrease during most of the remaining part of the year. Because most of the precipitation in the Mekong basin falls during the monsoon, a net increase in precipitation is predicted by all four models. Note that the HCCPR-CM3 model predicts a strong drying in the Amazon river basin during the second half of the year, resulting in a 9.8% decrease in annual precipitation volume.

3.2. STREAMFLOW CHANGES

Figures 6 and 7 show the mean monthly simulated hydrographs for the nine basins, both for the baseline conditions and the four climate models for 2025 and 2045, respectively. Although there is a large spread in predicted outcomes for most of the rivers, some general patterns are apparent.

The Yellow River in Southeast Asia was the only river for which a reduction in annual streamflow resulted for all of the climate models in both decades, even the MPI-ECHAM4 model in 2045, which predicted an increase in annual precipitation

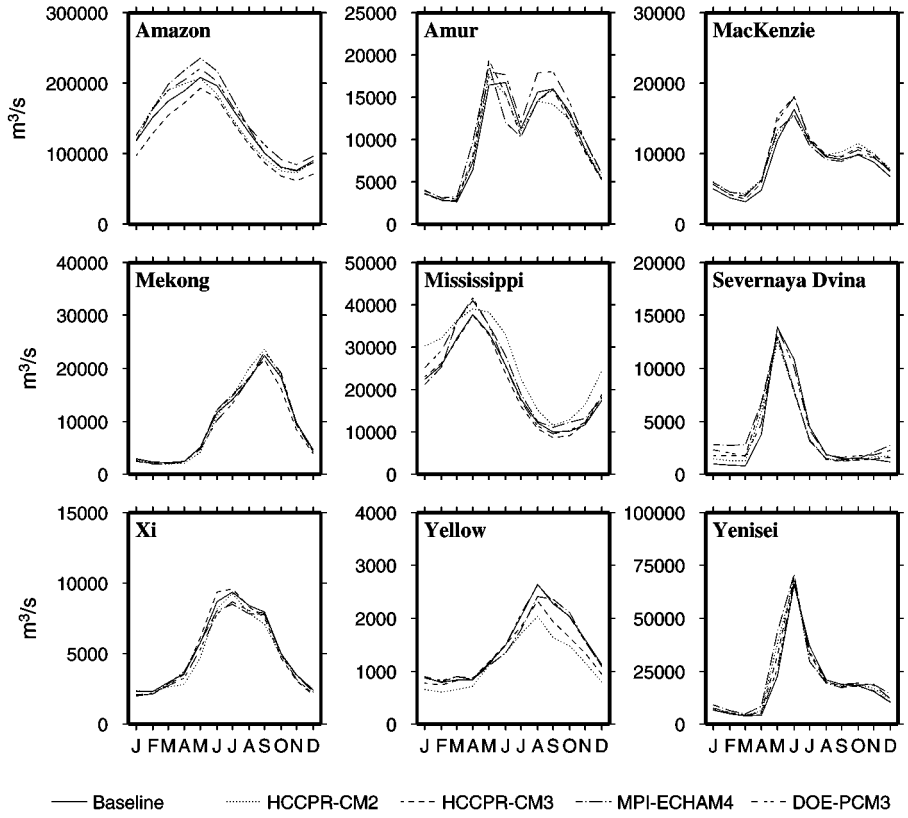

Figure 6. Mean monthly hydrographs for the nine basins for the baseline and climate model simulations in 2020–2029.

of 7.0% (from 517 to 553 mm). In this case, the increase in precipitation was offset by an increase in annual evapotranspiration of 9.3% (from 410 mm to 448 mm), caused by an increase in annual temperature of 2.7 °C. Consequently, the VIC model predicted a small decrease in annual runoff of 1% (from 106 to 105 mm).

The tropical and mid-latitude basins generally do not show a change in the seasonal hydrographs, other than a general wetting or drying, depending on whether the change in temperature and the resulting increase in evapotranspiration are sufficient to offset the increase in precipitation. The exception is the HCCPR-CM2 simulation for the Xi river basin in 2045, which shows a large reduction in streamflow during the second half of the year, resulting from a 22% reduction in precipitation (from 649 to 508 mm) during the last six months of the year.

One of the most persistent features of the predicted seasonal hydrographs occurs for those river basins in which a significant part of the annual precipitation falls in the form of snow under current climate conditions (Yenisei: 52%, Severnaya Dvina: 48%, Mackenzie: 41%, Amur: 21%). As mentioned in the previous section, the predicted warming in these high-latitude basins is greatest during the winter

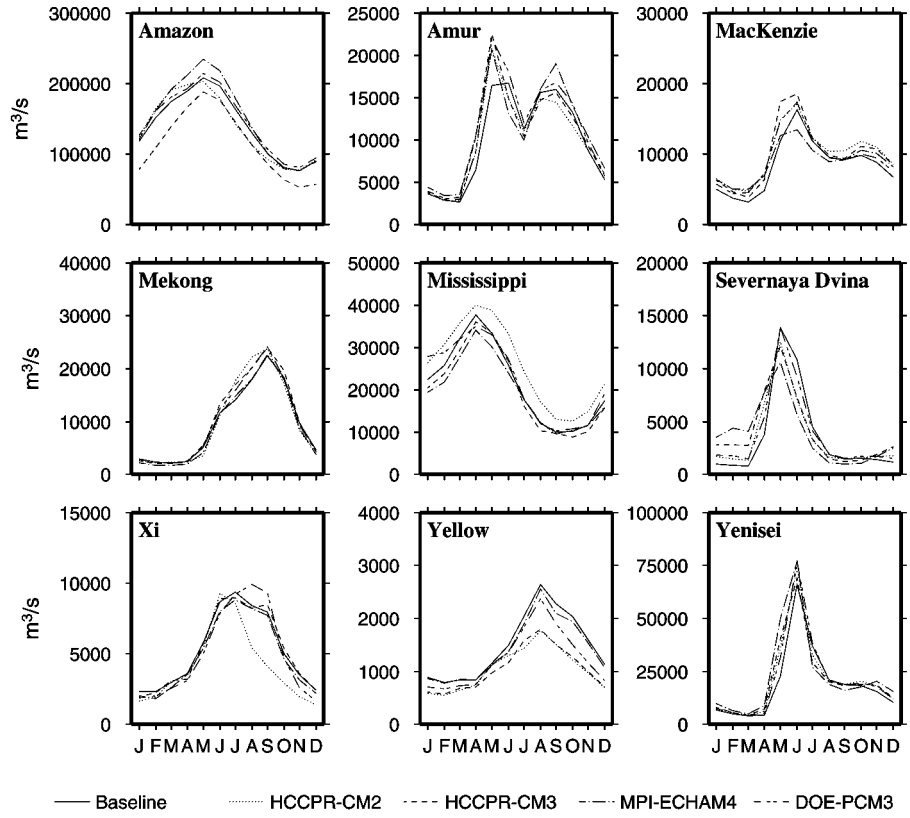

Figure 7. Mean monthly hydrographs for the nine basins for the baseline and climate model simulations in 2040–2049.

months. Consequently, a smaller amount of precipitation falls in the form of snow in the altered climate scenarios. This effect is most pronounced for those basins with large areas where the temperature is close to 0 °C during part of the winter. For instance, the reduction in the amount of the precipitation falling in the form of snow is greater in the Severnaya Dvina than in either the Yenisei or the Mackenzie river basins, both of which experience very low temperatures during the winter. The reduction in the proportion of precipitation falling as snow for the Severnaya Dvina in 2045 ranges from 9.9% (HCCPR-CM2) to 14.7% (MPI-ECHAM4). In comparison, the reduction in snow in the Yenisei ranges from 0.0% (DOE-PCM3) to 2.9% (HCCPR-CM3). This reduction in the amount of precipitation falling as snow leads to higher streamflows during the winter months, particularly in the Severnaya Dvina and to a lesser extent in the Mackenzie, Amur and Yenisei River basins.

In addition to a reduction in the amount of precipitation falling as snow, the start of snow accumulation is delayed and the onset of the snow melt is advanced as winter temperatures warm. Again, this is most pronounced for basins such as

the Severnaya Dvina, where temperatures are not as cold as in the Yenisei or Mackenzie basins. For all basins where a significant part of the precipitation is stored as snow during the winter months, the hydrographs increase earlier in the spring under the altered climate scenarios. However, the warmer basins, such as the Severnaya Dvina, show a decrease in the spring peak flows despite an increase in winter precipitation as a result of shallower snow packs. The cold basins on the other hand show an increase in the spring peak flows, because almost all of the increase in winter precipitation is stored as snow during the winter months. Maximum basin-wide snow accumulation in the Severnaya Dvina decreases from 313 mm water equivalent in April under current climate conditions to maximum accumulation in 2045 ranging from 164 mm in March (MPI-ECHAM4) to 264 mm in March (DOE-PCM3). In contrast, maximum accumulation in the Yenisei river basin increases from 210 mm in April under current conditions to maximum accumulation in 2045 ranging from 217 mm in April (HCCPR-CM3) to 237 mm in April (MPI-ECHAM4). Mid-latitude basins (Mississippi and Yellow) also show a significant decrease in the amount of precipitation falling as snow.

3.3. WATER BALANCE CHANGES

The monthly water balance for a river basin is given by

$$P_t = E_t + R_t + \Delta S_t \,, \tag{1}$$

where P_t is precipitation during month t, E is evapotranspiration, R is runoff, and ΔS is the change in storage, including water stored as soil moisture, snow, and canopy interception. All terms in Equation (1) are understood to be basin averages. Figure 8 shows each of the monthly water balance components from Equation (1) under current climate conditions. Note that the runoff in Equation (1) and Figure 8 is not the routed runoff in the channel network, but is the runoff generated at the grid cell level by the VIC model. Although these two quantities are identical when integrated over a sufficiently long period, they differ in their timing.

In the tropical river basins, precipitation and evapotranspiration are largely in phase, because enough energy is available for evaporation during most months. In the mid and high latitude basins, evapotranspiration peaks in early summer, when high soil moisture coincides with long days. Evapotranspiration tends to decrease in mid to late summer when moisture shortages stress the vegetation.

Storage changes tend to be largest in the snow dominated basins. For example, the total storage in the Severnaya Dvina River basin during May decreases by 109 mm. This is the net effect of an increase in soil moisture storage of 31 mm and a decrease in snow water equivalent of 141 mm. On the other hand, the storage change in June of 115 mm is the net effect of a decrease in soil moisture of 104 mm and a decrease of snow water equivalent of 10 mm. Storage changes in these basins are positive in the fall and winter, when soil moisture is replenished and water is stored as snow, and negative in spring and summer, when snow melt and evapotranspiration deplete the moisture storage.

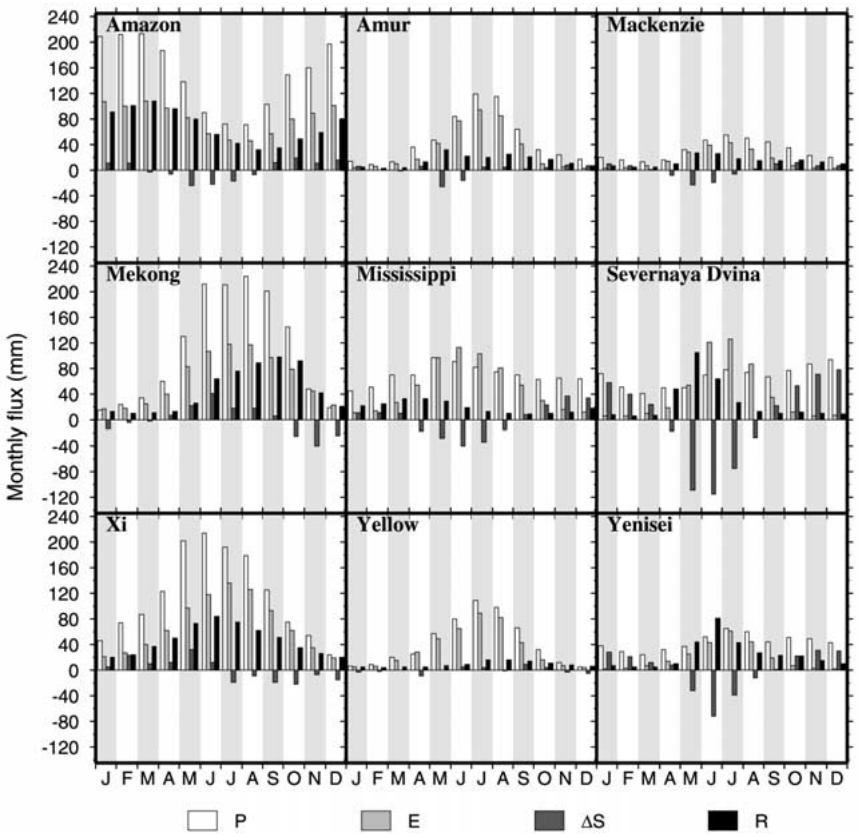

Figure 8. Mean monthly water balance components for current climate conditions for the nine river basins. Averages are for the period 1980–1993.

Figure 9 shows the change in the mean monthly water balance components for the DOE-PCM3 scenario in 2045. The DOE-PCM3 scenario was selected, because the associated hydrographs are generally representative of the changes predicted by the other models (see Figures 6 and 7). Temperature changes from the DOE-PCM3 model tend to be somewhat smaller than for the other models, with annual basinwide temperature changes in 2045 ranging from 1.1 °C for the Yenisei to 1.9 °C for the Mackenzie. Annual precipitation changes in 2045 range from –0.8% for the Xi to 7.7% for the Amur River basin.

In the Amazon basin a positive change in both precipitation and temperature is translated into an increase in evapotranspiration and runoff in most months. The Mekong and the Xi river basins, both in Southeast Asia, exhibit an increase of precipitation during the early part of the monsoon season and a decrease during the last part of the monsoon and during the dry season. Both runoff and evaporation are increased during most months with increased precipitation. However, much of the increased precipitation during the early part of the monsoon season is used to

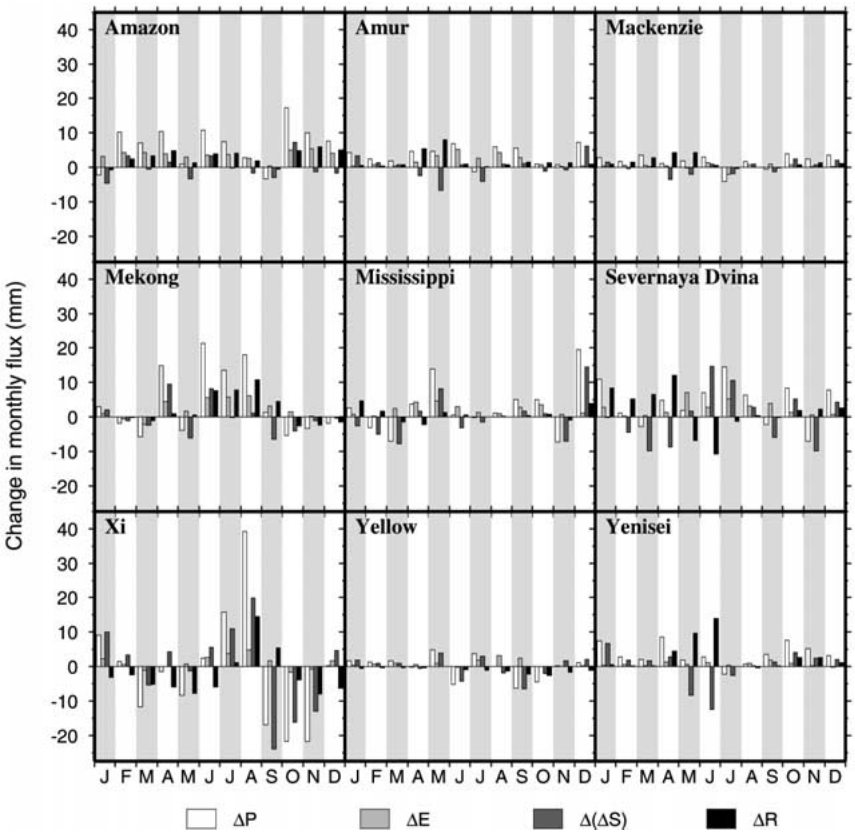

Figure 9. Predicted changes in the monthly water balance components in 2045 for the DOE-PCM3 scenario.

replenish soil moisture storage. Changes in the amount of water that enters or is released from soil moisture storage are particularly large in the Xi basin, which according to the DOE-PCM3 model, will experience the largest absolute changes in precipitation (increase of 39 mm in August and a decrease of 22 mm in both October and November).

Among the snow-dominated basins, the coldest basins again show a different signal as compared to the warmer basins. For the coldest basins (Amur, Mackenzie, and Yenisei) an increase in moisture storage is predicted during the winter months, because most of the increased precipitation is stored as snow. Consequently, snowmelt runoff is increased. In the warmer basins (Severnaya Dvina and Mississippi) snow water storage decreases, resulting in increased runoff during the winter, but decreased runoff during the snowmelt period.

4. Sensitivity Study

Diagnosis of the results presented in the previous section provides insight into the causes of changes in the hydrographs associated with the four different climate models. Nonetheless, it is difficult to analyze the hydrologic processes that are responsible for some of the changes in the water balance components, both because the climate models predict simultaneous changes in precipitation and temperature, and because there can be large month-to-month variations in the changes (even in their direction).

To isolate processes that lead to changes in the water balance components, we performed a controlled model experiment, in which temperature and precipitation were increased by fixed amounts for specified periods. Temperature was increased by 2 °C during each of the four seasons, here defined as December–February (DJF), March–May (MAM), June–August (JJA), and September–November (SON). Separately, the precipitation was increased by 10% during each of these four seasons as well. The results of this sensitivity experiment provide the basis for the interpretations in the following two sections.

4.1. SEASONAL CHANGE IN TEMPERATURE

Figure 10 shows the change in seasonal evapotranspiration in response to an increase in mean monthly temperature of 2 °C. The seasons along the abscissa represent the seasons during which the change in temperature was imposed, while the seasons along the ordinate axis correspond to the seasons for which the resulting change in the evapotranspiration was calculated. Thus, in Figure 10, circles along the diagonal represent changes in evapotranspiration during the same season in which the change in temperature was imposed. Off diagonal circles represent changes in season Y due to a change in temperature in season X. The area of the circles represents the magnitude of the relative change in the evapotranspiration, with black representing an increase and gray a decrease in evapotranspiration. Similarly, Figure 11 shows the relative change in runoff resulting from the same increase in temperature. Note that the circles represent percentage changes relative to the base case and that the scale of the circles is the same in both Figures 10 and 11.

For example, the panels for the Severnaya Dvina indicate that a 2° increase in temperature in the winter (DJF), leads to an increase in winter evapotranspiration of more than 10%, followed by a small increase in spring (MAM) evapotranspiration (Figure 10). The same temperature increase in the fall (SON) leads to an increase in fall runoff, but to an even greater relative increase in winter runoff (Figure 11). In contrast, a temperature increase in the summer (JJA) results in a decrease in runoff in all seasons for this basin (Figure 11).

The black circles on the main diagonal in Figure 10 indicate that an increase in temperature leads to an increase in evapotranspiration in the season in which the

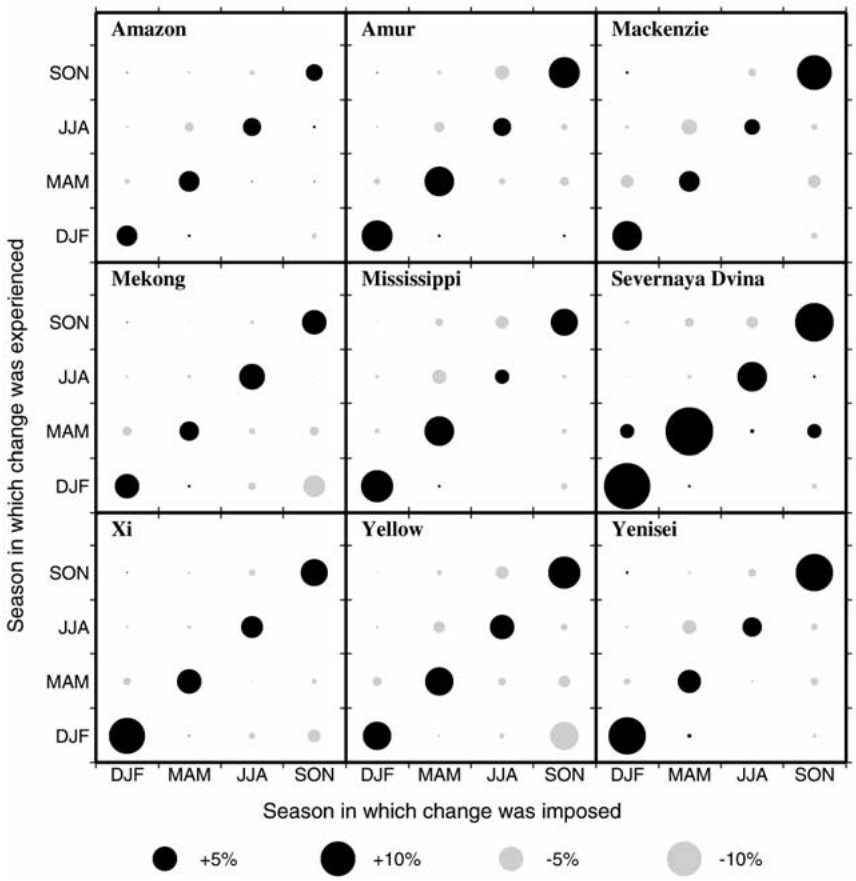

Figure 10. Relative change in seasonal evapotranspiration due to an increase in mean monthly temperature of 2 °C. The seasons along the abscissa represent the seasons during which the change in temperature was imposed, while the seasons along the ordinate axis correspond to the seasons for which the resulting change in the evapotranspiration was calculated. The magnitude of the relative change is indicated by the area of the circle, with black representing an increase and gray a decrease in evapotranspiration (see text for details).

temperature is increased. Note that because the circles represent relative changes, the large changes during the winter in the cold climates represent only a small absolute increase in evapotranspiration. In most cases the increase in evapotranspiration during the months in which the temperature is increased is accompanied by a decrease in evapotranspiration during the remaining months, because without a simultaneous increase in precipitation less water remains in storage and moisture stress is increased. This effect is strongest in the season immediately following the season in which the temperature change is imposed, and generally decreases for the seasons after that. The only exception to this is in the Severnaya Dvina basin, where an increase in temperature during the fall (SON) or winter (DJF)

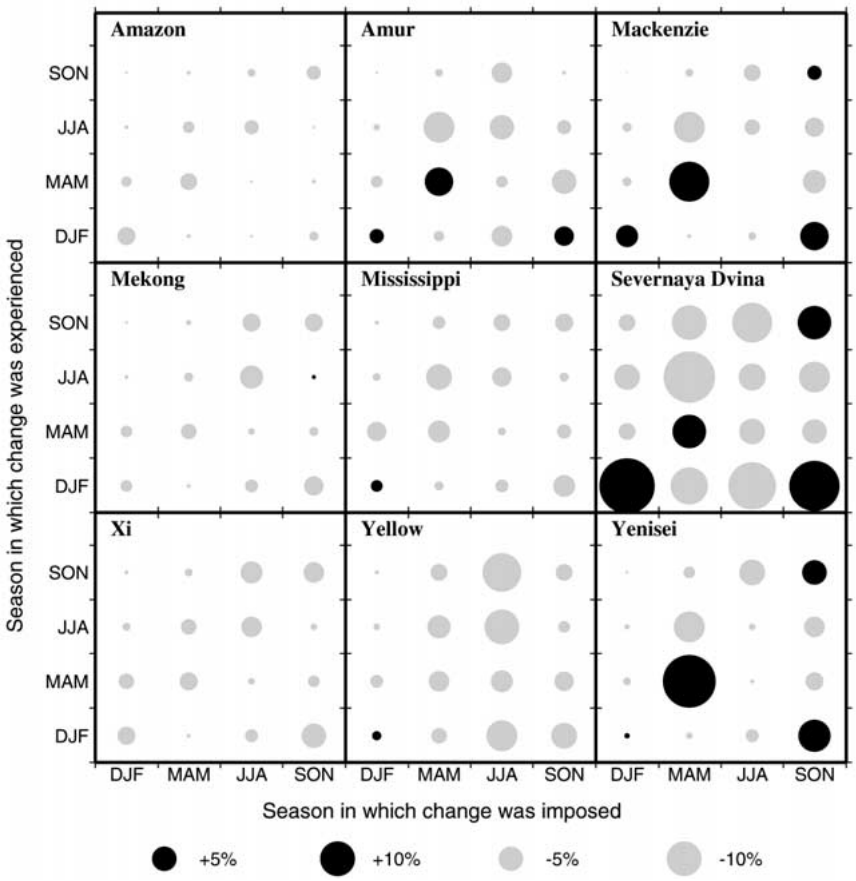

Figure 11. Relative change in seasonal runoff due to an increase in mean monthly temperature of 2 °C. For details see Figure 10 and the text.

leads to an increase in evapotranspiration during the spring (MAM) as well. In this case, a larger proportion of the precipitation in the fall and winter falls as rain, leading to reduction in the depth of the snow pack. In turn, the number of snow free days in May (defined as the area-weighted sum of snow free days per grid cell), increases by about one day. This leads to an increase in transpiration of about 1.5 mm (in the VIC model the vegetation does not transpire when snow is on the ground or in the canopy). Some of the basins also show a very small increase in evapotranspiration during the season preceding the season in which the temperature increase was imposed. These changes do not appear to be significant, because in all cases their magnitude is much less than 1 mm over a period of three months.

Figure 11 shows that increases in temperature generally lead to decreases in runoff, commensurate with the increases in evapotranspiration shown in Figure 10. The only cases where an increase in temperature leads to an increase in runoff is during the winter and spring months in those basins where water stored as

snow forms a significant component of the water balance. In the coldest basins (Yenisei, Mackenzie, and Amur) the greatest change occurs during MAM, because the temperature during DJF remains well below 0 °C, even with an increase of 2 °C. In contrast, the change in runoff in the Severnaya Dvina basin is more evenly distributed over the fall, winter and spring months.

4.2. SEASONAL CHANGE IN PRECIPITATION

Increasing precipitation increases both evapotranspiration (Figure 12) and runoff (Figure 13). Relative changes in runoff are generally larger than relative changes in evapotranspiration. To some extent, this can be explained because runoff forms a smaller component of the water balance than evapotranspiration, and an increase in both of 10 mm will result in a greater relative change in runoff. However, because the relative changes are different, the relative importance of runoff in the water balance increases. Because evapotranspiration is energy-limited during the winter months in the snow dominated basins, evapotranspiration in the winter increases only slightly in response to increases in precipitation during that period. The evapotranspiration in those basins responds much more strongly in summer, when sufficient energy is available to evaporate much of the extra precipitation. In the coldest basins the runoff change resulting from a winter increase in precipitation is largest in spring and summer, because most of the winter precipitation is stored as snow.

In the Severnaya Dvina river basin evapotranspiration decreases in the season after increasing the precipitation. In particular, evapotranspiration during the spring decreases, following an increase in precipitation during the fall and winter. The mechanism is the same as described in the previous section. Increased precipitation during the fall or winter leads to a thicker snow pack and reduces the number of snow free days during the spring, resulting in a small reduction of total evaporation during these three months.

4.3. OBSERVED TRENDS IN STREAMFLOW

Lins and Slack (1999), in a study of streamflow trends in the United States during the period 1944–1993, noted that trends were most prevalent in the annual minimum to median flows and least prevalent in the annual maximum category. Generally, increases in streamflow were observed across most of the United States, except in the Southeast and the Pacific Northwest, where decreases were observed. They concluded that the conterminous United States is becoming wetter and less extreme. Gan (1998) in a study of the Canadian Prairies, found that over the last 40–50 years many stations observed positive trends in streamflow during March, attributed to an earlier onset of snowmelt, followed by lower flows in May and june. This shift in streamflow is similar to the response of the Mackenzie and Severnaya Dvina we predict for an increase in temperature during the winter months (Figure 11). Similarly, Grabs et al. (2000) found a positive trend in the annual discharge

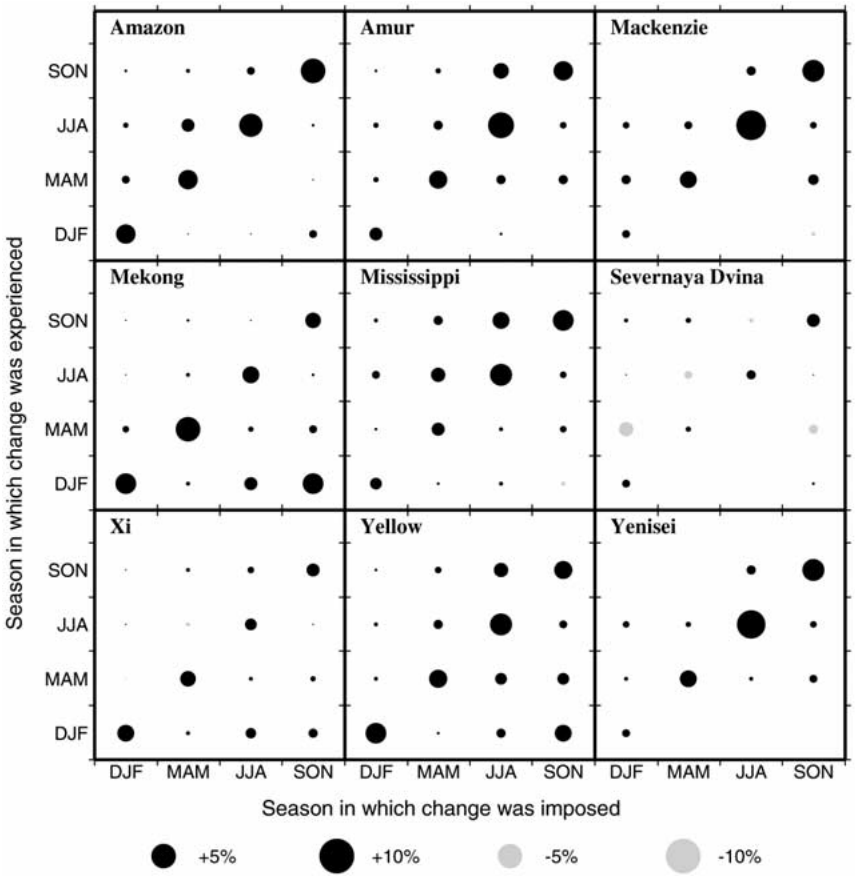

Figure 12. Relative change in seasonal evapotranspiration due to an increase in mean monthly precipitation of 10%. For details see Figure 10 and the text.

time series of Siberian rivers, with negative trends in the summer, and a positive trend during winter and early spring. Those observed trends are likewise similar to the signature we predict for warmer winter temperatures. Analysis of the annual streamflow of large rivers in southeastern South America for the period 1911–1993 (Robertson and Mechoso, 1998), showed an upward trend in the Paraguay-Paraná, especially since about 1960. The same trend was observed by Genta et al. (1998), who also noted that the amplitude of the seasonal cycle had decreased. Marengo et al. (1998) showed that variations in streamflow in Amazonia were strongly related to El Niño, but found no significant trends to wetter or drier conditions. The observed changes in South American rivers are consistent with our results in that changes in precipitation have an immediate and strong effect on streamflow (Figure 13).

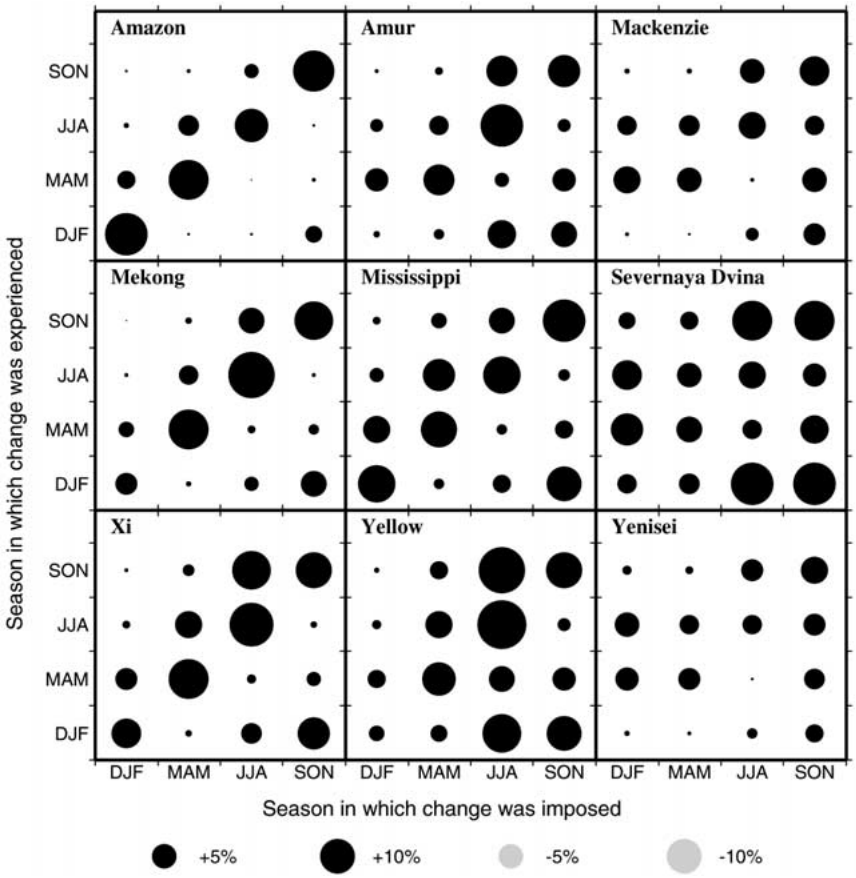

Figure 13. Relative change in seasonal runoff due to an increase in mean monthly precipitation of 10%. For details see Figure 10 and the text.

5. Changes in Drought Statistics

Because existing water resource management systems and ecosystems have developed to cope with current streamflow rates and volumes (and their variability), both increases and decreases in streamflow can have adverse effects. Increases in the length and intensity of droughts are of particular concern, because of globally increasing water supply demands (e.g., Vörösmarty et al., 2000). Floods, which are relatively short-term phenomena, are difficult to represent adequately given the monthly timestep of the flow data available to us. In addition, a different type of study would be required to examine the effects of changes in extreme precipitation, which are often the cause of floods.

A metric that can be used to assess the hydrologic vulnerability of a river basin is the average deficit length (L), that is, the average number of consecutive years that the annual river discharge is unable to meet a certain demand level (D). In

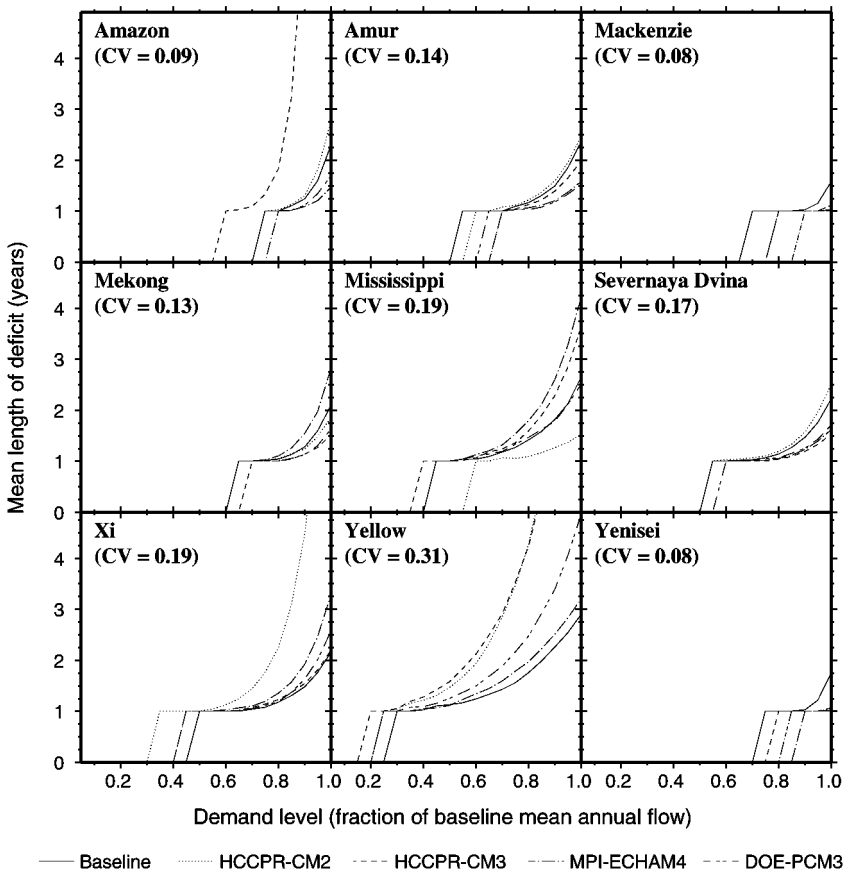

Figure 14. Mean deficit length as a function of the demand level for the nine basins (CV is coefficient of variation of the annual flow in the baseline simulation). Climate change simulations are based on 2045.

addition to the deficit length, other metrics such as the deficit magnitude and deficit intensity can be used. The magnitude M is defined as the cumulative excursion below D during the period of length L ($M = \sum_{t=1}^{L}(D - Q_t)$, with Q_t the annual flow during year t), and the intensity (I) is defined as $I = M/L$ (Salas, 1993).

Figure 14 shows the mean deficit length as a function of the demand level for each of the nine basins in 2045. The demand level is here defined as a fraction of the baseline mean annual flow. Because the entire analysis period from the model simulations comprises only 14 years (the first year is a spin up year and is not used in the analysis), the following method was used in the construction of Figure 14. A two-parameter log-normal distribution was fitted to each of the annual flow series of each simulation. To this end, the annual series were log-transformed and normalized, resulting in normally distributed series with a mean of zero and a standard deviation of one. A lag one autoregressive model (AR(1)) was fitted to

each of the annual series, and a 10,000 year series of annual flows was generated using the AR(1) model (Salas, 1993). These 10,000 year time series were then used to calculate the mean deficit lengths plotted in Figure 14. The demand level was defined as a fraction of the baseline mean annual flow and increased in steps of 5% between 5% and 100% of the baseline mean annual flow.

Arguably, a 14 year time series will in most cases be insufficient to fit an AR(1) model and derive reliable statistics. However, in this case we are concerned with a change in the mean deficit length as a function of a change in climate, in order to evaluate the change in vulnerability of the different basins. Because we are only interested in changes relative to the base case, we argue that even though the actual numbers may be open to discussion, the qualitative changes in the vulnerability reflected by the curves in Figure 14 are informative.

The range of the baseline curves in Figure 14 reflects the coefficient of variation (CV) of the annual flows (the coefficient of variation of a statistical sample is defined as the standard deviation divided by the mean). The arctic rivers and the Amazon have the lowest CV (Mackenzie and Yenisei: CV = 0.08, Amazon: CV = 0.09), while the Yellow shows the highest CV (CV = 0.31).

An upward shift of the curves in Figure 14 reflects a drying of the basin, because the average deficit length increases for the same demand level. A downward shifts corresponds to a decrease of the average deficit length for a given demand level, and consequently represents a wetting of the basin. As seen before, all models predict a drying in the Yellow River basin in 2045, with the largest degree of drying predicted by the two Hadley Centre models. The Xi also becomes drier, with only one model (HCCPR-CM2) predicting a large change. Two models predict an increase in runoff in the Amazon, one predicts a slight decrease, while the HCCPR-CM3 model predicts a large increase in the mean deficit length. The high latitude basins generally become wetter. For these basins, the increase in temperature during the winter months contributes only slightly to an increase in evapotranspiration, and much of the increased precipitation consequently contributes to an increase in runoff. The signals for the Mekong and Mississippi are mixed.

Figure 14 shows the extent of disagreement in the regional simulations that still exists between the various GCMs. Whereas HCCPR-CM2 predicts the greatest drying in the Amazon and MPI-ECHAM4 predicts the greatest wetting, this signal is reversed in the Mississippi, where MPI-ECHAM4 predicts the greatest wetting and HCCPR-CM2 the greatest drying.

6. Conclusions

Transient climate predictions from four GCMs were used to assess the hydrologic sensitivity to climate change of nine large, continental river basins. The GCMs were selected because they have modern land surface schemes, high spatial resolutions, and generally represent the current state-of-the-art in climate simulations.

All of the models used either the IPCC IS92a emission scenario, or a 1% compound annual increase in CO_2. The nine river basins represent a range of geographic and climatic conditions. Changes in basinwide, mean annual temperature and precipitation were calculated for three decades in the transient climate model runs (2025, 2045, and 2095) and hydrologic model simulations were performed for decades centered on 2025 and 2045. In addition, sensitivity analyses were performed in which temperature and precipitation were increased independently by 2 °C and 10%, respectively, during each of four seasons.

The main conclusions of this study are:

- All models predict a warming for all nine basins, but the amount of warming varies widely between the models, especially with increased time horizon. The greatest warming is predicted to occur during the winter months in the highest latitudes. Precipitation generally increases, but the monthly precipitation signal varies more between the models than does temperature.
- The largest changes in the hydrological cycle are predicted for the snow-dominated basins of mid to higher latitudes. Partly, this is a result of the greater amount of warming that is predicted for these regions. More importantly, though, the presence or absence of snow fundamentally changes the nature of the land surface water balance, because of the effect of water storage in the snow pack. Water stored as snow during the winter does not become available for runoff or evapotranspiration until the following spring's melt period. Because of this cumulative process, the snow pack integrates the effects of climate change over a period of months, and the largest hydrological changes are manifested in the early to mid spring melt period. In general, the streamflow regime in snowmelt dominated basins is most sensitive to increases in temperature during the winter months.
- Somewhat different sensitivities to climate warming are predicted for the coldest snow dominated basins than for transitional basins. Whereas the former show an increase of the spring streamflow peak in response to warmer temperatures and increased winter precipitation, the latter show a decrease. In the coldest basins, any increase in precipitation during the winter is stored as snow, because even for a relatively large increase in temperature, winters will remain quite cold with temperatures generally well below freezing. In contrast, in the warmer basins increased temperature leads to increased rainfall during the winter and a decrease in the depth of the snow pack. The net effect is that the spring snow melt peak is reduced.
- Globally, the hydrological response predicted for most of the basins in response to the GCMs predictions is a reduction in annual streamflow in the tropical and mid-latitudes. In contrast, high-latitude basins tend to show an increase in annual runoff, because most of the predicted increase in precipitation occurs during the winter, when the available energy is insufficient for an

increase in evaporation. Instead, water is stored as snow and contributes to an increase in streamflow during the following snow melt period.

Acknowledgement

This work was supported by the U.S. Environmental Protection Agency under STAR Grant R 824802-01-0 to the University of Washington.

References

Abdulla, F. A., Lettenmaier, D. P., Wood, E. F., and Smith, J. A.: 1996, 'Application of a Macroscale Hydrologic Model to Estimate the Water Balance of the Arkansas-Red River Basin', *J. Geophys. Res.* **101**, 7449–7459.

Arnell, N. W.: 1999a, 'The Effect of Climate Change on Hydrological Regimes in Europe: A Continental Perspective', *Global Environ. Change* **9**, 5–23.

Arnell, N. W.: 1999b, 'Climate Change and Global Water Resources', *Global Environ. Change* **9**, S31–S49.

Batjes, N. H.: 1995, *A Homogenized Soil Data File for Global Environmental Research: A Subset of FAO, ISRIC and NCRS Profiles*, Technical Report, International Soil Reference and Information Centre (ISRIC), Wageningen.

Battisti, D. and Sarachik, E.: 1995, 'Understanding and Predicting ENSO', *Rev. Geophys.* **33**, 1367–1376.

Boer, G. J., Flato, G., and Ramsden, D.: 2000a, 'A Transient Climate Change Simulation with Greenhouse Gas and Aerosol Forcing: Projected Climate to the Twenty-First Century, *Clim. Dyn.* **16**, 427–450.

Boer, G. J., Flato, G., Reader, M. C., and Ramsden, D.: 2000b, 'A Transient Climate Change Simulation with Greenhouse Gas and Aerosol Forcing: Experimental Design and Comparison with the Instrumental Record for the Twentieth Century', *Clim. Dyn.* **16**, 405–425.

Bras, R. A.: 1990, *Hydrology, an Introduction to Hydrologic Science*, Addison Wesley, Inc., Reading, MA.

Chao, P.: 1999, 'Great Lakes Water Resources: Climate Change Impact Analysis with Transient GCM Scenarios', *J. Amer. Water Resour. Assoc.* **35**, 1485–1499.

Cherkauer, K. A. and Lettenmaier, D. P.: 1999, 'Hydrologic Effects of Frozen Soils in the Upper Mississippi River Basin', *J. Geophys. Res.* **104**, 19,599–19,610.

Cosby, B. J., Hornberger, G. M., Clapp, R. B., and Ginn, T. R.: 1984, 'A Statistical Exploration of the Relationships of Soil Moisture Characteristics to the Physical Properties of Soils', *Water Resour. Res.* **20**, 682–690.

Doherty, R. and Mearns, L.: 1999, *A Comparison of Simulations of Current Climate from Two Coupled Atmosphere-Ocean Global Climate Models against Observations and Evaluation of their Future Climates*, Report to the National Institute for Global Environmental Change, Technical Report, NCAR.

Emori, S., Nozawa, T., Abe-Ouchi, A., Numaguti, A., Kimoto, M., and Nakajima, T.: 1999, 'Coupled Ocean-Atmosphere Model Experiments of Future Climate Change with an Explicit Representation of Sulfate Aerosol Scattering', *J. Meteorol. Soc. Japan* **77**, 1299–1307.

FAO: 1995, *The Digital Soil Map of the World*, version 3.5.

Felzer, B. and Heard, P.: 1999, 'Precipitation Differences amongst GCMs Used for the U.S. National Assessment', *J. Amer. Water Resour. Assoc.* **35**, 1327–1340.

Frederick, K. D. and Schwarz, G. E.: 1999, 'Socioeconomic Impacts of Climate Change on U.S. Water Supplies, *J. Amer. Water Resour. Assoc.* **35**, 1563–1584.

Gan, T. Y.: 1998, 'Hydroclimatic Trends and Possible Climatic Warming in the Canadian Prairies', *Water Resour. Res.* **34**, 3009–3015.

Genta, J. L., Perez-Iribarren, G., and Mechoso, C. R.: 1998, 'A Recent Increasing Trend in the Streamflow of Rivers in Southeastern South America', *J. Climate* **11**, 2858–2862.

Glanz, M., Katz, R., and Nicholls N. (eds.): 1991, *Teleconnections Linking Worldwide Climate Anomalies*, Cambridge University Press, Cambridge, U.K.

Gleick, P. H.: 1999, 'Studies from the Water Sector of the National Assessment', *J. Amer. Water Resour. Assoc.* **35**, 1297–1300.

Gleick, P. H. and Chalecki, E. L.: 1999, 'The Impacts of Climatic Changes for Water Resources of the Colorado and Sacramento-San Joaquin River Basins', *J. Amer. Water Resour. Assoc.* **35**, 1429–1442.

Gordon, C., Cooper, C., Senior, C., Banks, H., Gregory, J., Johns, T., Mitchell, J., and Wood, R.: 2000, 'The Simulation of SST, Sea Ice Extents and Ocean Heat Transports in a Version of the Hadley Centre Coupled Model without Flux Adjustments', *Clim. Dyn.* **16**, 147–168.

Gordon, H. B. and O'Farrell, S. P.: 1997, 'Transient Climate Change in the CSIRO Coupled Model with Dynamic Sea Ice', *Mon. Wea. Rev.* **125**, 875–907.

Grabs, W. E., Portmann, F., and De Couet, T.: 2000, 'Discharge Observation Networks in Arctic Regions: Computation of the River Runoff into the Arctic Ocean, Its Seasonality and Variability', in Lewis, E. L., Jones, E. P., Lemke, P., Prowse, T. D., and Wadhams, P. (eds.), *The Freshwater Budget of the Arctic Ocean*, NATO ARW, Kluwer Academic Publishers, Dordrecht, pp. 249–267.

Graham, S. T., Famiglietti, J. S., and Maidment, D. R.: 1999, '5-Minute, 1/2°, and 1° Data Sets of Continental Watersheds and River Networks for Use in Regional and Global Hydrologic and Climate System Modeling Studies', *Water Resour. Res.* **35**, 583–587.

Hamlet, A. F. and Lettenmaier, D. P.: 1999, 'Effects of Climate Change on Hydrology and Water Resources in the Columbia River Basin', *J. Amer. Water Resour. Assoc.* **35**, 1597–1623.

Hansen, M. C., DeFries, R. S., Townshend, J. R. G., and Sohlberg, R.: 2000, 'Global Land Cover Classification at 1 km Spatial Resolution Using a Classification Tree Approach', *Int. J. Remote Sens.* **21**, 1331–1364.

Huffman, G. J. et al.: 1997, 'The Global Precipitation Climatology Project (GPCP) Combined Precipitation Dataset', *Bull. Amer. Meteorol. Soc.* **78**, 5–20.

Hughes, J., Lettenmaier, D., and Guttorp, P.: 1993, 'A Stochastic Approach for Assessing the Effects of Changes in Regional Circulation Patterns on Local Precipitation', *Water Resour. Res.* **29**, 3303–3315.

Hulme, M.: 1995, 'Estimating Global Changes in Precipitation', *Weather* **50**, 34–42.

IPCC: 1996, *Climate Change 1995: The Science of Climate Change*, Cambridge University Press, Cambridge, U.K.

Johns, T. C., Carnell, R. E., Crossley, J. F., Gregory, J. M., Mitchell, J. F. B., Senior, C. A., Tett, S. F. B., and Wood, R. A.: 1997, 'The Second Hadley Centre Coupled Ocean-Atmosphere GCM: Model Description, Spinup and Validation', *Clim. Dyn.* **13**, 103–134.

Jones, P. D.: 1994, 'Hemispheric Surface Air Temperature Variations: A Reanalysis and an Update to 1993', *J. Climate* **7**, 1794–1802.

Kalnay, E. et al.: 1996, 'The NCEP/NCAR 40-Year Reanalysis Project', *Bull. Amer. Meteorol. Soc.* **77**, 437–471.

Kimball, J. S., Running, S. W., and Nemani, R. R.: 1997, 'An Improved Method for Estimating Surface Humidity from Daily Minimum Temperature', *Agric. For. Meteorol.* **85**, 87–98.

Kirschbaum, M. U. F., Evans, J. R., Goulding, K., Jarvis, P. G., Noble, I. R., Rounsevell, M., and Sharkey, T. D.: 1996, 'Ecophysiological, Ecological, and Soil Processes in Terrestrial Ecosystems: A Primer on General Concepts and Relationships', in Watson, R. T., Zinyowera, M. C., and Moss, R. H. (eds.), *Climate Change 1995: Impacts, Adaptations and Mitigation of Climate*

Change: Scientific-Technical Analyses; Contribution of Working Group II to the Second Assessment Report of the Intergovernmental Panel on Climate Change, Cambridge University Press, Cambridge, U.K.

Lettenmaier, D. P. and Gan, T. Y.: 1990, 'Hydrologic Sensitivities of the Sacramento-San Joaquin River Basin, California, to Global Warming', *Water Resour. Res.* **26**, 69–86.

Lettenmaier, D. P., Wood, A. W., Palmer, R. N., Wood, E. F., and Stakhiv, E. Z.: 1999, 'Water Resources Implications of Global Warming: A U.S. Regional Perspective', *Clim. Change* **43**, 537–579.

Leung, L. R. and Wigmosta, M. S.: 1999, 'Potential Climate Change Impacts on Mountain Watersheds in the Pacific Northwest', *J. Amer. Water Resour. Assoc.* **35**, 1463–1472.

Leung, L. R., Hamlet, A. F., Lettenmaier, D. P., and Kumar, A.: 1999, 'Simulations of the ENSO Hydroclimate Signals in the Pacific Northwest Columbia River Basin', *Bull. Amer. Meteorol. Soc.* **80**, 2313–2329.

Liang, X., Lettenmaier, D. P., and Wood, E. F.: 1996, 'One-Dimensional Statistical Dynamic Representation of Subgrid Spatial Variability of Precipitation in the Two-Layer Variable Infiltration Capacity Model', *J. Geophys. Res.* **101**, 21,403–21,422.

Liang, X., Lettenmaier, D. P., Wood, E. F., and Burges, S. J.: 1994, 'A Simple Hydrologically Based Model of Land Surface Water and Energy Fluxes for General Circulation Models', *J. Geophys. Res.* **99**, 14,415–14,428.

Lins, H. F. and Slack, J. R.: 1999, 'Streamflow Trends in the United States', *Geophys. Res. Lett.* **26**, 227–230.

Lohmann, D., Nolte-Holube, R., and Raschke, E.: 1996, 'A Large-Scale Horizontal Routing Model to Be Coupled to Land Surface Parametrization Schemes', *Tellus* **48A**, 708–721.

Lohmann, D., Raschke, E., Nijssen, B., and Lettenmaier, D. P.: 1998a, 'Regional Scale Hydrology: I. Formulation of the VIC-2L Model Coupled to a Routing Model', *Hydrol. Sci. J.* **43**, 131–141.

Lohmann, D., Raschke, E., Nijssen, B., and Lettenmaier, D. P.: 1998b, 'Regional Scale Hydrology: II. Application of the VIC-2L Model to the Weser River, Germany', *Hydrol. Sci. J.* **43**, 143–158.

Manabe, S., Stouffer, R. J., Spelman, M. J., and Bryan, K.: 1991, 'Transient Responses of a Coupled Ocean-Atmosphere Model to Gradual Changes of Atmospheric CO_2, Part I: Annual Mean Response', *J. Climate* **4**, 785–818.

Marengo, J., Tomasella, J., and Uvo, C. R.: 1998, 'Trends in Streamflow and Rainfall in Tropical South America: Amazonia, Eastern Brazil, and Northwestern Peru', *J. Geophys. Res.* **103**, 1775–1783.

Matheussen, B., Kirschbaum, R. L., Goodman, I. A., O'Donnell, G. M., and Lettenmaier, D. P.: 2000, 'Effects of Land Cover Change on Streamflow in the Interior Columbia River Basin (U.S.A. and Canada)', *Hydrol. Process.* **14**, 867–885.

Melillo, J. M., Prentice, I. C., Farquhar, G. D., Schulze, E.-D., and Sala, O. E.: 1996, 'Terrestrial Biotic Responses to Environmental Change and Feedbacks to Climate', in Houghton, J. T., Meira Filho, L. G., Callander, B. A., Harris, N., Kattenberg, A., and Maskell, K. (eds.), *Climate Change 1995: The Science of Climate Change; Contribution of Working Group I to the Second Assessment Report of the Intergovernmental Panel on Climate Change*, Cambridge University Press, Cambridge, U.K., pp. 445–481.

Miller, N., Kim, J. H. R. K., and Farrara, J.: 1999, 'Downscaled Climate and Streamflow Study of the Southwestern United States', *J. Amer. Water Resour. Assoc.* **35**, 1525–1538.

Nicholls, N., Gruza, G. V., Jouzel, J., Karl, T. R., Ogallo, L. A., and Parker, D. E.: 1996, 'Observed Climate Variability and Change', in Houghton, J. T., Meira Filho, L. G., Callander, B. A., Harris, N., Kattenberg, A., and Maskell, K. (eds.), *Climate Change 1995: The Science of Climate Change; Contribution of Working Group I to the Second Assessment Report of the Intergovernmental Panel on Climate Change*, Cambridge University Press, Cambridge, U.K., pp. 133–192.

Nijssen, B., Lettenmaier, D. P., Liang, X., Wetzel, S. W., and Wood, E. F.: 1997, 'Streamflow Simulation for Continental-Scale River Basins', *Water Resour. Res.* **33**, 711–724.

Nijssen, B., O'Donnell, G. M., Lettenmaier, D. P., Lohmann, D., and Wood, E. F.: 2001a, 'Predicting the Discharge of Global Rivers', *J. Climate*, accepted.

Nijssen, B., Schnur, R., and Lettenmaier, D. P.: 2001b, 'Global Retrospective Estimation of Soil Moisture Using the VIC Land Surface Model, 1980–1993', *J. Climate* **14**, 1790–1808.

Ojima, D., Garcia, L., Elgaali, E., Miller, K., Kittel, T. G. F., and Lackett, J.: 1999, 'Potential Climate Change Impacts on Water Resources in the Great Plains', *J. Amer. Water Resour. Assoc.* **35**, 1443–1455.

Olsen, J., Stedinger, J., Matalas, N., and Stakhiv, E.: 1999, 'Climate Variability and Flood Frequency Estimation for the Upper Mississippi and Lower Missouri Rivers', *J. Amer. Water Resour. Assoc.* **35**, 1509–1523.

Robertson, A. W. and Mechoso, C. R.: 1998, 'Interannual and Decadal Cycles in River Flows of Southeasterm South America', *J. Climate* **11**, 2570–2581.

Röckner, E., Bengtsson, L., Feichter, J., Lelieveld, J., and Rodhe, H.: 1999, 'Transient Climate Change Simulations with a Coupled Atmosphere-Ocean GCM Including the Tropospheric Sulfur Cycle', *J. Climate* **12**, 3004–3032.

Röckner, E. et al.: 1996, *The Atmospheric General Circulation Model ECHAM-4: Model Description and Simulation of Present-Day Climate*, Technical Report 218, Max-Planck-Institut für Meteorologie, Hamburg, Germany.

Row, L. W., Hastings, D. A., and Dunbar, P. K.: 1995, *TerrainBase Worldwide Digital Terrain Data Documentation Manual*, National Geophysical Data Center, Boulder, CO.

Salas, J. D.: 1993, 'Analysis and Modeling of Hydrologic Time Series', in Maidment, D. R. (ed.), *Handbook of Hydrology*, McGraw-Hill Inc., New York, pp. 19.1–19.72.

Simpson, H., Cane, M., Lin, S., Zebiak, S., and Herczeg, A.: 1993, 'Forecasting Annual Discharge of River Murray, Australia, from a Geophysical Model of Enso', *J. Climate* **6**, 386–390.

Stouffer, R. J. and Manabe, S.: 1999, 'Response of a Coupled Ocean-Atmosphere Model to Increasing Atmospheric Carbon Dioxide: Sensitivity to the Rate of Increase', *J. Climate* **12**, 2224–2237.

Thiaw, W. M., Barnston, A. G., and Kumar, V.: 1999, 'Predictions of African Rainfall on the Seasonal Timescale', *J. Geophys. Res.* **104**, 31,589–31,597.

Thornton, P. E. and Running, S. W.: 1999, 'An Improved Algorithm for Estimating Incident Daily Solar Radiation from Measurements of Temperature, Humidity, and Precipitation', *Agric. For. Meteorol.* **93**, 211–228.

Vörösmarty, C. J., Fekete, B. M., and Tucker, B. A.: 1998, 'Global River Discharge Database (RivDis) v. 1.1', online at http://www-eosdis.ornl.gov or on CD-ROM from the ORNL Distributed Active Archive Center, Oak Ridge National Laboratory, Oak Ridge, TN, U.S.A.

Vörösmarty, C. J., Green, P., Salisbury, J., and Lammers, R. B.: 2000, 'Global Water Resources: Vulnerability from Climate Change and Population Growth', *Science* **289**, 284–288.

Washington, W. M. et al.: 2000, 'Parallel Climate Model (PCM) Control and Transient Simulations', *Clim. Dyn.* **16**, 755–774.

Wolock, D. and McCabe, G.: 1999, 'Estimates of Runoff Using Water-Balance and Atmospheric General Circulation Models', *J. Amer. Water Resour. Assoc.* **35**, 1341–1350.

Wood, E. F., Lettenmaier, D. P., Liang, X., Nijssen, B., and Wetzel, S. W.: 1997, 'Hydrological Modeling of Continental-Scale Basins', *Ann. Rev. Earth Pl. Sc.* **25**, 279–300. Also appeared in Dietrich, W. E. and Sposito, G. (eds.), *Hydrological Processes, from Catchment to Continental Scales*, Annual Reviews, Palo Alto, CA, pp. 313–336.

(Received 20 April 2000; in revised form 9 January 2001)